



Effect of dissolved oxygen on L-methionine production from glycerol by *Escherichia coli* W3110BL using metabolic flux analysis method

Kun Niu^{1,2} · Yue-Ying Xu^{1,2} · Wang-Jie Wu^{1,2} · Hai-Yan Zhou^{1,2} · Zhi-Qiang Liu^{1,2} · Yu-Guo Zheng^{1,2}

Received: 10 December 2019 / Accepted: 30 January 2020 / Published online: 12 February 2020
© Society for Industrial Microbiology and Biotechnology 2020

Abstract

L-Methionine is an essential amino acid in humans, which plays an important role in the synthesis of some important amino acids and proteins. In this work, metabolic flux of batch fermentation of L-methionine with recombinant *Escherichia coli* W3110BL was analyzed using the flux balance analysis method, which estimated the intracellular flux distributions under different dissolved oxygen conditions. The results revealed the producing L-methionine flux of 4.8 mmol/(g cell·h) [based on the glycerol uptake flux of 100 mmol/(g cell·h)] was obtained at 30% dissolved oxygen level which was higher than that of other dissolved oxygen levels. The carbon fluxes for synthesizing L-methionine were mainly obtained from the pathway of phosphoenolpyruvate to oxaloacetic acid [15.6 mmol/(g cell·h)] but not from the TCA cycle. Hence, increasing the flow from phosphoenolpyruvate to oxaloacetic acid by enhancing the enzyme activity of phosphoenolpyruvate carboxylase might be conducive to the production of L-methionine. Additionally, pentose phosphate pathway could provide a large amount of reducing power NADPH for the synthesis of amino acids and the flux could increase from 41 mmol/(g cell·h) to 51 mmol/(g cell·h) when changing the dissolved oxygen levels, thus meeting the requirement of NADPH for L-methionine production and biomass synthesis. Therefore, the following modification of the strains should be based on the improvement of the key pathway and the NAD(P)/NAD(P)H metabolism.

Keywords *Escherichia coli* · L-Methionine · Dissolved oxygen · Metabolic flux · NAD(P)/NAD(P)H metabolism

Introduction

L-methionine (L-MET), containing proteinogenic amino acids with cysteine, is an essential amino acid for humans and animals [16, 31]. L-MET also plays an important role as a methyl donor and metabolic intermediate in vivo in

the synthesis of S-adenosyl-methionine (SAM), polyamine and lipoic acid [27]. L-MET can be obtained by chemical resolution from DL-methionine or enzymatic process from the precursors D-5-(2-methylthion-ethyl)-hydantoin [15] or O-succinyl-L-homoserine [12]. However, the chemical or enzymatic method is harmful to the environment and the cost is too high [21–23, 27]. By comparison, fermentative production of L-MET by genetic engineering bacteria is an environment friendly way and has been explored over the past few decades. Usuda et al. reported that recombinant *E. coli* W3110 could produce 0.24 g/L L-MET from glucose in 500 mL flask for 48 h [34]. Another *E. coli* Me05 improved L-MET production to 5.62 g/L in 15 L fermenter from glucose [17]. Also, a strain of *Streptomyces* sp. SP-05 was found to produce 3.72 g/L MET in culture broth from sucrose [37]. However, there was very little focus on the central metabolism genetic interventions for improving L-MET production. In our previous study, a series of L-MET-producing strains had been constructed and one strain could produce 9.75 g/L L-MET with the productivity of 0.20 g/L/h from glucose in a 5 L bioreactor, which is the highest reported ever [10].

Electronic supplementary material The online version of this article (<https://doi.org/10.1007/s10295-020-02264-w>) contains supplementary material, which is available to authorized users.

✉ Zhi-Qiang Liu
microlu@zjut.edu.cn

¹ The National and Local Joint Engineering Research Center for Biomufacturing of Chiral Chemicals, Zhejiang University of Technology, Hangzhou 310014, People's Republic of China

² Key Laboratory of Bioorganic Synthesis of Zhejiang Province, College of Biotechnology and Bioengineering, Zhejiang University of Technology, No. 18 Chaowang Road, Hangzhou 310014, Zhejiang Province, People's Republic of China

Although the effect of different culture conditions, such as dissolved oxygen (DO), pH or different carbon sources, on L-MET production had already been investigated, the metabolism mechanism under different culture conditions was still unknown. Metabolic flux is generally considered to be a fundamental determinant of the metabolic phenotype, which represents the result of nonlinear interactions among proteins, metabolic concentrations and genes. Therefore, the quantification of carbon flux distribution plays an important role in understanding and analyzing the complex interactions between genotypic changes and corresponding phenotypic responses [13, 43, 46].

Metabolic flux analysis could help to calculate or evaluate the yield of intermediates and it could also predict differences in flow distribution between different strains. Metabolic flux analysis mainly includes ^{13}C labeling, stoichiometric metabolite balancing, and constraint-based approaches like flux balance analysis (FBA) [4]. Michael et al. showed great uncertainties in carbon metabolism on malate degradation from glycerol in *E. coli* by flux variability analysis and enabled further characterization of L-phenylalanine production through constructing a series of malic enzyme mutants [36]. Another report indicated that FBA was a mathematical approach to analyze the flux of metabolites by a metabolic network to enhance the production of succinate and lactate in *E. coli* [3]. Niu et al. estimated the undeterminable intermediate metabolites of uptake hydrogen inside the cell during the hydrogen production and the results showed the different culture conditions had significant effects on hydrogen production [30]. FBA was also performed for *Clostridium sporogenes* NCIM 2918 grown on different carbon sources with varied concentrations, which revealed that the mixture carbon source was useful for cell growth as well as the alcohol biosynthesis [13].

In aerobic bioprocesses, the growth of the microorganisms, maintenance, metabolism, and product yield were significantly affected by DO levels [1, 40, 41]. The DO level had an important influence on the biomass, the plasmid content, and the recombinant protein levels of recombinant *E. coli* at the stationary phase. NADH/NAD⁺ ratio would also be changed under different DO levels, as well as the glycolysis rate, substrate and energy metabolism, and cellular redox balance [33]. Several researches reported that there was a relationship between the NAD(P)H/NAD(P)⁺ ratios and the metabolic flux distributions under aerobic/anaerobic conditions with *Azotobacter vinelandii* [5]. In our previous research, L-MET was synthesized with various recombinant *E. coli* under different culture conditions, including the pH, DO level and initial glycerol concentration [10, 11]. However, the metabolic flux under different conditions was still unknown, so the influence mechanism of these culture conditions on L-MET was not clear. For this purpose, an appropriate quantitative model to simulate

the metabolic flux was established. The metabolic network of recombinant *E. coli* involving the L-MET pathway under the aerobic conditions with glycerol was constructed. FBA method was used to explore the effect of DO levels on intracellular flux, particularly L-MET production and by-product flows, which would help us to understand the impact mechanism of these culture conditions on L-MET production and provide a reference for subsequent optimization of molecular and engineering strategies.

Materials and methods

Strains and medium

The bacterial strain used in this study was *E. coli* W3110 $\Delta metJ \Delta metI \Delta lysA$ Trc-*metH* Trc-*metF* Trc-*cysE* Trc-*metBL/pTrc99A/metA*/yjeH* (*E. coli* W3110BL), which was constructed by our lab [10]. The recombinant strain was derived from several genetic modifications of the L-MET production strain *E. coli* W3110. Luria-Bertani (LB) medium was used for seed cultures which contained 10 g/L tryptone, 5 g/L yeast extract, and 10 g/L NaCl. L-MET fermentation was conducted in MS medium and the medium component optimization was done before, which contained 45 g/L glycerol, 12 g/L $(\text{NH}_4)_2\text{SO}_4$, 2 g/L yeast extract, 2 g/L KH_2PO_4 , 7 g/L $\text{Na}_2\text{S}_2\text{O}_3$, 1 mg/L VB_{12} , and 1 mL/L salt solution ($\text{MgSO}_4 \cdot 7\text{H}_2\text{O}$ 0.5 g/L, $\text{MnSO}_4 \cdot 8\text{H}_2\text{O}$ 5 mg/L, $\text{FeSO}_4 \cdot 7\text{H}_2\text{O}$ 5 mg/L, and ZnSO_4 5 mg/L) [31].

Cultivation conditions

Batch fermentation experiments were performed in a 5 L bioreactor (working volume 3 L, stirred by a mechanical agitator at 300 rpm). Seed cultures for fermentation were grown by transferring fresh colonies to a 200 mL flask containing 50 mL LB medium at 37 °C. After incubation for 12 h, seed liquid was inoculated into 5 L bioreactor containing 3 L cultivation media [35]. Cell was grown at 30 °C and 300 rpm with 1.0 vvm air delivery and 50 mg/mL ampicillin was required to maintain plasmid retention. Since the strains were L-lysine auxotrophic mutants, L-lysine with final concentration of 1 g/L was added into the fermentation broth. When the optical density at 600 nm reached about 0.6, a final concentration of 0.05 mM isopropyl- β -D-thiogalactopyranoside (IPTG) was added to the medium for induction. The speed of agitator and ventilation rate were used to keep dissolved oxygen (DO) at 10%, 30% and 50% if necessary and the floating range of the DO value does not exceed 5%. The pH was controlled at 7.0 by addition of either H_3PO_4 or $\text{NH}_3 \cdot \text{H}_2\text{O}$. Fermentation of different culture conditions was conducted simultaneously for at least three times [48].

Theory of FBA

FBA is a modeling tool which involved the reconstruction of metabolic network. The metabolic grid contains the necessary biochemical reactions and then a mathematical representation of the stoichiometric coefficients of each reaction in the form of a matrix called stoichiometric model. And the metabolic flux was estimated by these coefficients through the metabolic network. The metabolic network consisted of enzymatic reactions that facilitate the conversion of intracellular metabolism and exchange of metabolites with the extracellular environment. The transient behavior of these processes could be quantitatively described by formulating a dynamic mass balance over each intracellular metabolite pool. The metabolic flux analysis was based on the pseudo-steady-state hypothesis, which assumed that the change rate of the concentration of intermediate metabolites in the cell was zero, and n intermediate metabolites can obtain n constraints on the rate of change [25]. Supposing the total number of rates to be determined was J , then the degree of freedom for solving the problem was $F = J - n$. As long as the number of uncorrelated rates measured was not less than the degree of freedom F , the flux distribution of the entire metabolic network can be determined. Therefore, the following Eq. (1) was generated, which was used to describe the transient behavior of each metabolite [30]:

$$\frac{dX_i}{dt} = \sum_j S_{ij} V_j, \quad (1)$$

wherein V_j corresponded to the j th flux in the system; S_{ij} showed the number of moles of metabolite i produced or consumed in the reaction j ; X_i represented the concentration of the metabolite. In steady state, the concentration of metabolites in the network was constant, and Eq. (1) could be simplified into a set of linear homogeneous equations, which are written in the equation using matrix representation (2) [29]:

$$S \cdot v = 0. \quad (2)$$

Equation (2) expressed a group of steady-state metabolite balances, which were just linear combinations of reaction rates [30], where S was a stoichiometric matrix of dimensions $m \times n$ of stoichiometric coefficients containing m metabolites in n reactions, and v was a flow vector corresponding to the flow of n reactions [8, 29].

Metabolic network of *Escherichia coli* W3110BL

Escherichia coli can be developed to utilize various carbon sources for organic acid and amino acids production effectively for its clear inheritance background [18, 19].

Glycerol is a potential substrate for the production of amino acids, because of the higher reduced state [6, 28, 39]. Glycerol could be utilized by *E. coli* in both aerobic and anaerobic conditions, which contains glycerol dissimilation pathways, glycolytic pathway, pentose phosphate pathway (PP pathway), TCA cycle, amino acids biosynthesis pathway, anaplerosis pathway and respiratory chain, etc. In this study, only the metabolic pathways under aerobic condition were listed considering the DO conditions in the experiment. Glycerol is first transferred into DHAP after two steps of reaction by ATP-dependent glycerol kinase and NAD⁺-dependent G3P dehydrogenase, and then DHAP was transferred into GA-3P which was a reversible reaction by triose-phosphate isomerase. After a series of biochemical reactions, L-MET is finally produced [45]. The *E. coli* biomass composition was based on the previous report [7]. To facilitate calculation and analysis, the metabolic network of this study was simplified according to the previously reported method [29]: (1) since the carbon source in the medium is glycerol and the nitrogen source is an inorganic nitrogen source, the reaction pathways such as amino acid degradation reaction, nucleotide salvage pathway, and utilization reaction of other carbon sources are removed; (2) extraction of glycolytic pathway, PP pathway, TCA cycle, oxidative phosphorylation, major amino acid synthesis reaction in metabolic network; (3) cells are thought to consist of proteins, DNA, RNA, fatty acid, and cell walls, and the cell composition is normalized, and the synthesis of fatty acid and cell walls is expressed as a synthesis of precursors in a simplified metabolic network; and (4) since the lysine synthesis pathway of the strain was knocked out, the lysine synthesis branch was not considered. The metabolic network of *E. coli* W3110BL under aerobic glycerol fermentation is shown in Fig. 1, which was based on the KEGG metabolic pathway database and other publications. Abbreviations for the metabolites and related metabolic reactions are listed in Table S1 and Table S2, respectively.

Solution of the MFA models

In this study, a metabolic matrix which contained 43 metabolic reactions and 38 intracellular metabolites were constructed according to Fig. 1, and the model had a degree of freedom of 5. The specific rate for uptake glycerol (r_1) and the specific formation rate of formic acid, lactic acid, acetic acid, L-MET and succinate (r_{38} , r_{39} , r_{40} , r_{35} , and r_{18}) could be measured. Hence, the positive definite system could be solved by the software Matlab 2016a. All the flux distributions were normalized based on the specific uptake rate of glycerol of 100 mmol/(g cell^h) and expressed as percentage.

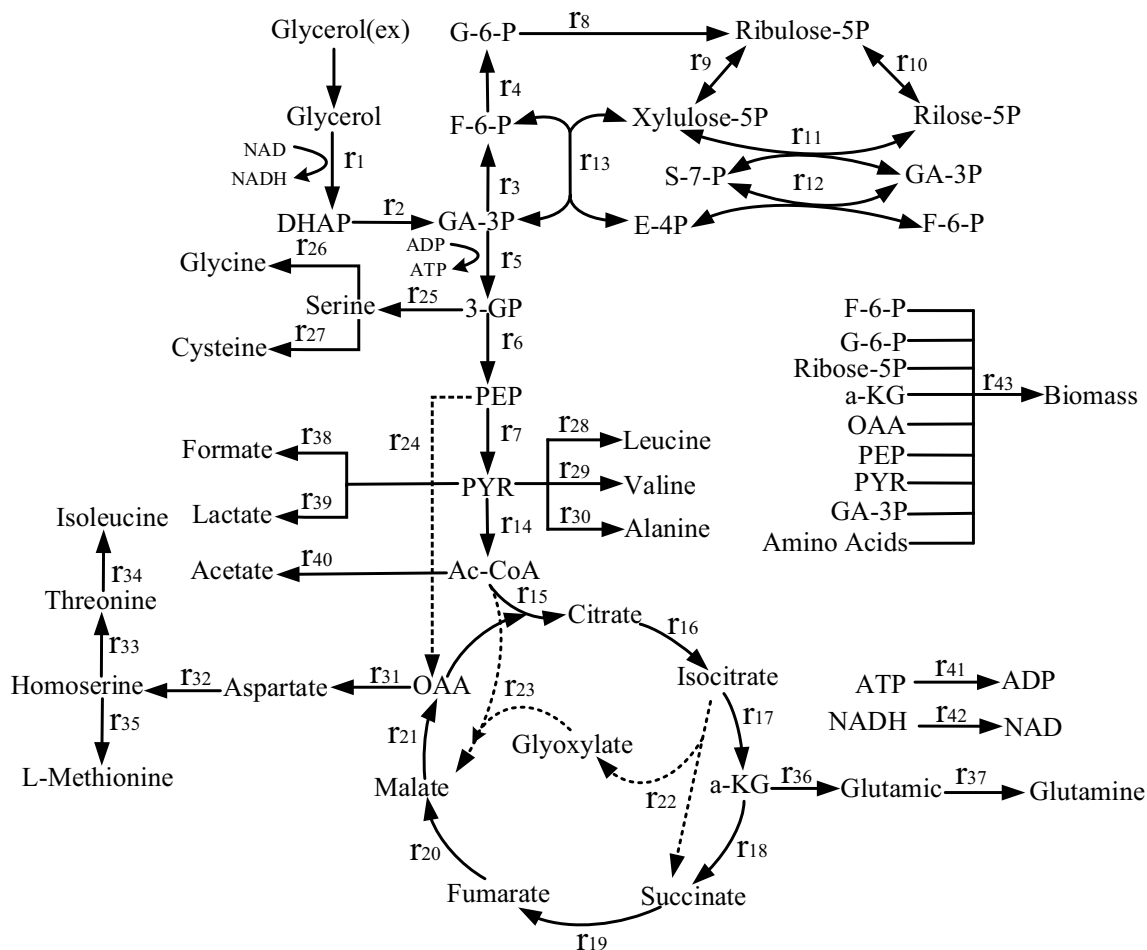


Fig. 1 Central carbon metabolic network of glycerol in *Escherichia coli* W3110BL under aerobic condition

Analytical methods

The optical density (OD) was measured at 600 nm and used as an estimate of cell mass. The extracellular concentrations of acetic acid, formic acid, succinate acid and lactic acid were determined by high-performance liquid chromatography (HPLC) equipped with a RI detector (Waters, Milford, MA, USA). Separation of metabolites was done by the Aminex HPX-87H column (Bio-Rad, Hercules, CA, USA) working at 35 °C with a constant flow rate of 0.6 mL/min (5 mM H₂SO₄).

The concentration of L-MET in the culture supernatant was determined by Agilent 1260 system HPLC (Agilent Technologies, Santa Clara, CA, USA) equipped with a UV detector working at 365 nm. A gradient of two mobile phases was applied for L-MET separating: eluent A 26.6 mM ammonium acetate and eluent B chromatographic grade methanol. After mixing A and B with 1:1 (v: v), acetic acid was added to keep the pH at 7.0. And, 10 µL of the sample was injected into the HPLC column (Unitary C₁₈

5 µm 100 A 250 mm × 4.6 mm) (Accheom, Wenling, China) at a column temperature of 40 °C and a constant flow rate of 1 mL/min [17].

Results and discussion

Growth characteristics of the L-methionine producing *E. coli* W3110BL

Escherichia coli showed various DO demands at different physiological stages, so higher or lower DO is unfavorable to the normal fermentation process. Under high dissolved oxygen conditions, the cells enter the decline phase in advance and the cells grow slowly under low dissolved oxygen conditions. In this study, the growth behaviors of the L-MET producing *E. coli* W3110BL under three different DO levels were investigated.

As shown in Fig. S1A and S1B, with the increase of DO concentration, the specific growth rate and biomass were

gradually increased at the early stage of the fermentation. The cell growth decreased under 50% DO condition at the stationary phase, which indicated that the metabolism of the microorganism was accelerated and the growth time was shortened at 50% DO condition, further reducing the production of the metabolites. Meanwhile, the results in Fig. S1B showed that the 10% DO level resulted in the lowest biomass production.

The production of L-MET in Fig.S1C showed the same trend as the cell growth. When DO was controlled at about 30%, the yield of L-MET was higher than that of the other two groups. The L-MET production under 50% DO was shown to be better than that of 30% at the lag phase, however, it continued to increase at the stationary phase at 30% DO condition and reached maximum. This maybe because the strains need more oxygen to grow at the early stage and then enter into a stable period with the growth, resulting in a decrease of respiratory rate and oxygen demand. Therefore, the cell growth and L-MET production were generally inhibited at lower DO concentrations, but a relatively higher DO concentration could result in the rapid growth of the strains and change of the metabolic flux, further reducing L-MET production. Under lower DO condition (10%), the concentration of lactic acid and acetic acid was higher than that of the other two groups (Fig. S1D). The concentration of lactic acid and acetic acid could reach about 2.45 g/L and 2.14 g/L, respectively, which were almost twice as that of the other two conditions. This may be due to the fact that lactate dehydrogenase (LDH) for the synthesis of lactic acid is more active under low DO condition [26]. The final production of acetic acid under different conditions was similar to that of lactic acid at the end of the fermentation, but the fermentation curve showed that the acetic acid was gradually increased in the early and middle stages of growth and then decreased. Therefore, during the fermentation process, part of acetic acid was used as the carbon source as the glycerol exhausted.

As an important intermediate metabolite, aspartic acid was a common precursor of L-MET, L-threonine and L-isoleucine. In this present study, L-aspartic acid, L-threonine and L-isoleucine reached 1.58, 1.89 and 1.51 g/L at 30% DO

condition, respectively. In addition, lower productivity of amino acid was obtained under a long-term low DO condition (10%), and the production of L-aspartic acid, L-threonine and L-isoleucine decreased by 26.6%, 34.9% and 23.2%, respectively, compared to the 30% DO condition. Table 1 showed some parameters at the exponential growth phase with different DO levels. With the increase of DO level from 10 to 50%, the specific growth rate of cells ($0.16\text{--}0.22\text{ h}^{-1}$) and the biomass yield $Y_{X/G}$ ($0.10\text{--}0.18\text{ g g glycerol}^{-1}$) were all increased. On the contrary, the specific uptake rate of glycerol was decreased, which may because of the reason that we mentioned above that more intermediate metabolite could be produced at higher DO level, then some of them, such as acetic acid, were consumed as the carbon source, thereby reducing the specific uptake rate of glycerol. At the same time, the specific rate of acetic acid formation had a significant decrease from 3.04 to 0.47 mmol/(g cell·h) with the increasing DO level, and acetic acid yield was fivefold lower under 30% DO ($0.02\text{ g g glycerol}^{-1}$) compared to that of 10% DO ($0.11\text{ g g glycerol}^{-1}$). When the DO exceeded 30%, the specific formation rate of acetic acid increased slightly, which indicated that both lower and higher DO would produce more acetic acid as reported in the previous research [1, 33]. The specific formation rate of L-MET was maximal at 10% DO [$0.52\text{ mmol}/(\text{g cell}\cdot\text{h})$], but the maximum yield $Y_{M/G}$ of $0.05\text{ g g glycerol}^{-1}$ was obtained at 30% DO level, which showed significant differences with the other two conditions (p value < 0.01). Therefore, the method of controlling DO levels in stages should be adopted to improve the fermentation efficiency of L-MET in the future experiments.

Effect of DO on central carbon metabolic fluxes

Estimation of carbon flux by FBA was achieved by maximizing or minimizing a biologically relevant objective with pseudo-steady-state approximation for the metabolites. Figure 2 indicated the central metabolic fluxes at different DO levels of 10–50%, including the glycolytic pathway, PP pathway, TCA cycle, the synthesis of amino acid, and the cofactor and ATP metabolism. At G-6-P node, the carbon flux of

Table 1 Exponential growth of the *E. coli* at different DO levels

DO level (%)	Specific growth rate (h^{-1})	Specific rate [mmol/(g cell·h)]			Yield (g g^{-1}) ^a		
		Glycerol uptake	L-Methionine formation	Acetate formation	$Y_{X/G}^b$	$Y_{M/G}$	$Y_{A/G}$
10	0.16 ± 0.015	18.13 ± 0.12	0.52 ± 0.028	3.04 ± 0.14	0.10 ± 0.01	0.05 ± 0.001	0.11 ± 0.01
30	0.20 ± 0.012	13.95 ± 0.11	0.44 ± 0.029	0.47 ± 0.03	0.13 ± 0.005	0.05 ± 0.001	0.02 ± 0.001
50	0.22 ± 0.016	10.23 ± 0.06	0.24 ± 0.013	0.53 ± 0.03	0.18 ± 0.005	0.04 ± 0.001	0.03 ± 0.001

^a $Y_{X/G}$ biomass yield on glycerol, $Y_{M/G}$ L-methionine yield on glycerol, $Y_{A/G}$ acetate yield on glycerol

^b p value < 0.01 , data not shown

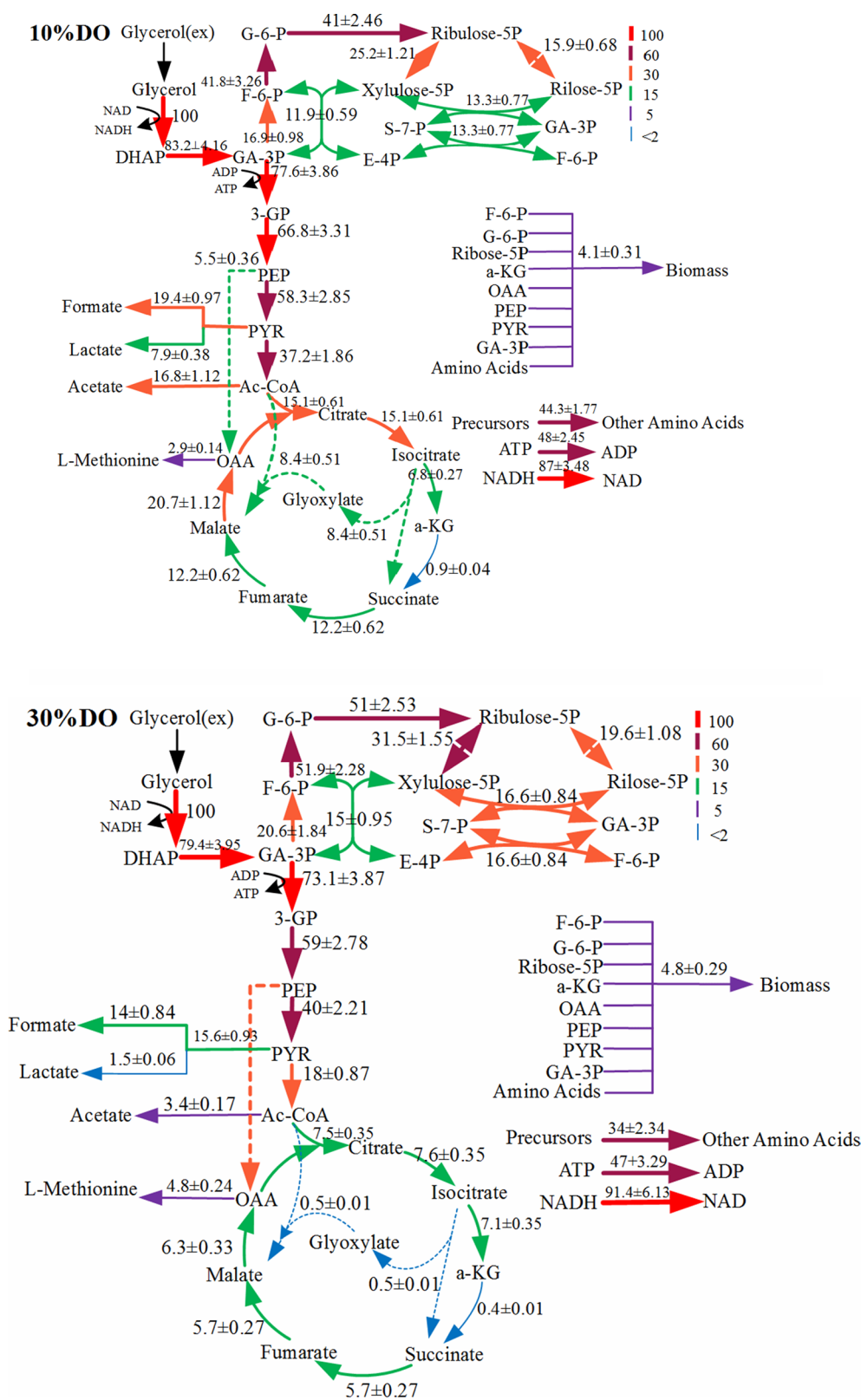


Fig. 2 Metabolic flux of glycerol in *E. coli* W3110BL under different DO levels. All the flux values are normalized to the specific uptake rate of glycerol of 100 mmol/(g cell·h)

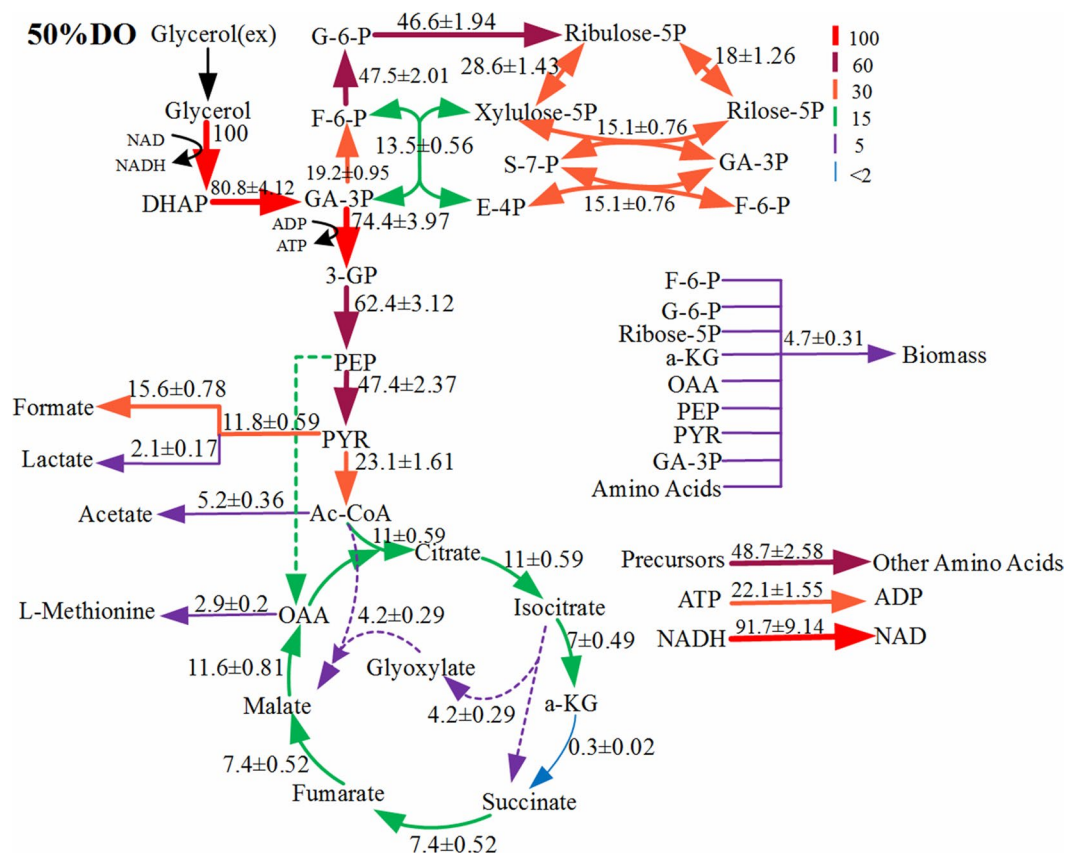


Fig. 2 (continued)

PP pathway and glycolytic pathway was affected markedly by DO levels. When the DO level was 10%, the flux of PP pathway was about 41%, but it would enhance to 51% as DO level increased to 30%. The PP pathway can provide a large amount of reducing power NADPH for amino acids synthesis and changing DO level leads to a redirection of carbon from glycolysis towards the PP pathway for increasing NADPH supply, and then meet the requirement of NADPH for the synthesis of biomass. Therefore, the increasing metabolic flux of the PP pathway benefited the improvement of the biosynthesis of L-MET, which was consistent with our experimental results [38]. However, under the 10% DO level condition, there was more carbon flux flow into 3-GP from GA-3P (Fig. 2), so the flux to glycolysis pathway decreased from 77.6 to 73.1% with the increase in DO levels from 10 to 30%. Ac-CoA is an important precursor for the synthesis of TCA cycle products, and the flux to Ac-CoA had a sharp decline from 37.2 to 18% with the increasing DO levels from 10 to 30%, and then back to 23.1% at 50% DO level. OAA was another key intermediate in the TCA cycle obtained from PEP. When the DO was controlled at 30%, the carbon flux of synthesizing L-MET was mainly obtained from the reaction of PEP to OAA but not from the TCA cycle (Fig. 2). Hence, increase of the PEP flow to the OAA was

more conducive to the target product L-MET. The reaction was catalyzed by phosphoenolpyruvate carboxylase (PEPC) which has been reported that overexpression of PEPC could enhance the production of malic acid in *E. coli* [24]. As an important intermediate of TCA cycle, malic acid is the precursor of OAA and the flux of OAA determines the flux to L-MET. Therefore, we suspected that DO levels might affect the activity of PEPC and then changed the metabolic flux of intermediates in the TCA cycle [20]. Thus, a proper increase of the DO level would allow more carbon flux from the replenishing pathway to the OAA and then improve the carbon flux to L-MET and reduce the flux to TCA cycle and by-product synthesis. Moreover, lower or higher DO had a negative effect on the flux of this reaction, which reduced 64.7% and 24.3% compared with that at 30% DO, respectively [2].

As for the synthesis of amino acids, the highest flux distribution to the goal product L-MET of 4.8% was obtained at 30% DO level, however, the flux to the other amino acids, mainly including glutamic, glutamine, serine and aspartate was highest at 48.7% when DO reached 50%. It has been reported in the literature that maintaining a high DO level during fermentation was beneficial to the production of glutamic acid [44]. From the results of metabolic flow, it

could be concluded that the synthesis of organic acids was affected obviously by the DO levels. When low DO of 10% was controlled, 16.8% carbon flux was used to synthesize acetic acid and it reduced to only 3.4% when DO increased to 30%. Similarly, the fluxes of influent formic acid and lactic acid were also lower at 30% DO. In addition, it showed during the late exponential growth phase, the carbon flux used for cell growth was almost the same at 30% (4.8%) and 50% DO (4.7%).

Cofactor NADH/NADPH and ATP metabolic flux under different DO conditions

The metabolism of the cofactor NADH/NADPH and the energy ATP was important for the fermentation process [47]. Energy ATP and NADH cooperated to visualize the process of intracellular biological reaction [47]. The NADH cofactor plays an important role in biological oxidation reduction reactions during catabolism, while NADPH plays a key role in biosynthetic anabolism reactions. Under aerobic condition, NADH is used as an electron donor for ATP production in the electron transport chain, which is used for reduced metabolites production under fermentation conditions [14]. The metabolic pathway of L-MET is similar to the formation of L-isoleucine, which needs 2 mol of NADPH from homoserine to synthesize 1 mol of L-MET. Many studies have shown that the L-isoleucine yield could be significantly enhanced by increasing the intracellular NADPH content. Therefore, the transformation of the coenzyme flow based on the analysis of the L-MET anabolic pathway may result in a significant increase in the yield of L-MET [32, 42].

It was reported that the metabolic balance of cofactors and energy can be assessed by metabolic flux [43]. In this metabolic pathway, NADPH was mainly produced by the reaction of glucose 6-phosphate dehydrogenase through the PP pathway. In addition, the NADPH-dependent isocitrate dehydrogenase in the TCA cycle can also catalyze the reversible conversion between NADH and NADPH [9, 43]. The formation of ATP was mainly formed by substrate-level phosphorylation (glycolysis, TCA cycle and acetate secretion pathway) and oxidative phosphorylation. The relative contribution of these pathways to NADPH/NADH production and ATP utilization of *E. coli* W3110BL under different DO conditions is shown in Fig. 3. The results in Fig. 3a indicated that NADH was mainly generated from the glycolysis pathway. With higher DO levels, the NADH produced by the glycolysis pathway was relatively reduced, suggesting that under hypoxic conditions, the intracellular NADH cannot be consumed in time by the respiratory chain and then accumulated in large quantities. Hence, the level of oxidative phosphorylation was theoretically relative lower. To provide enough ATP to satisfy the growth of the cells, the cells must undergo a large amount of substrate to synthesize

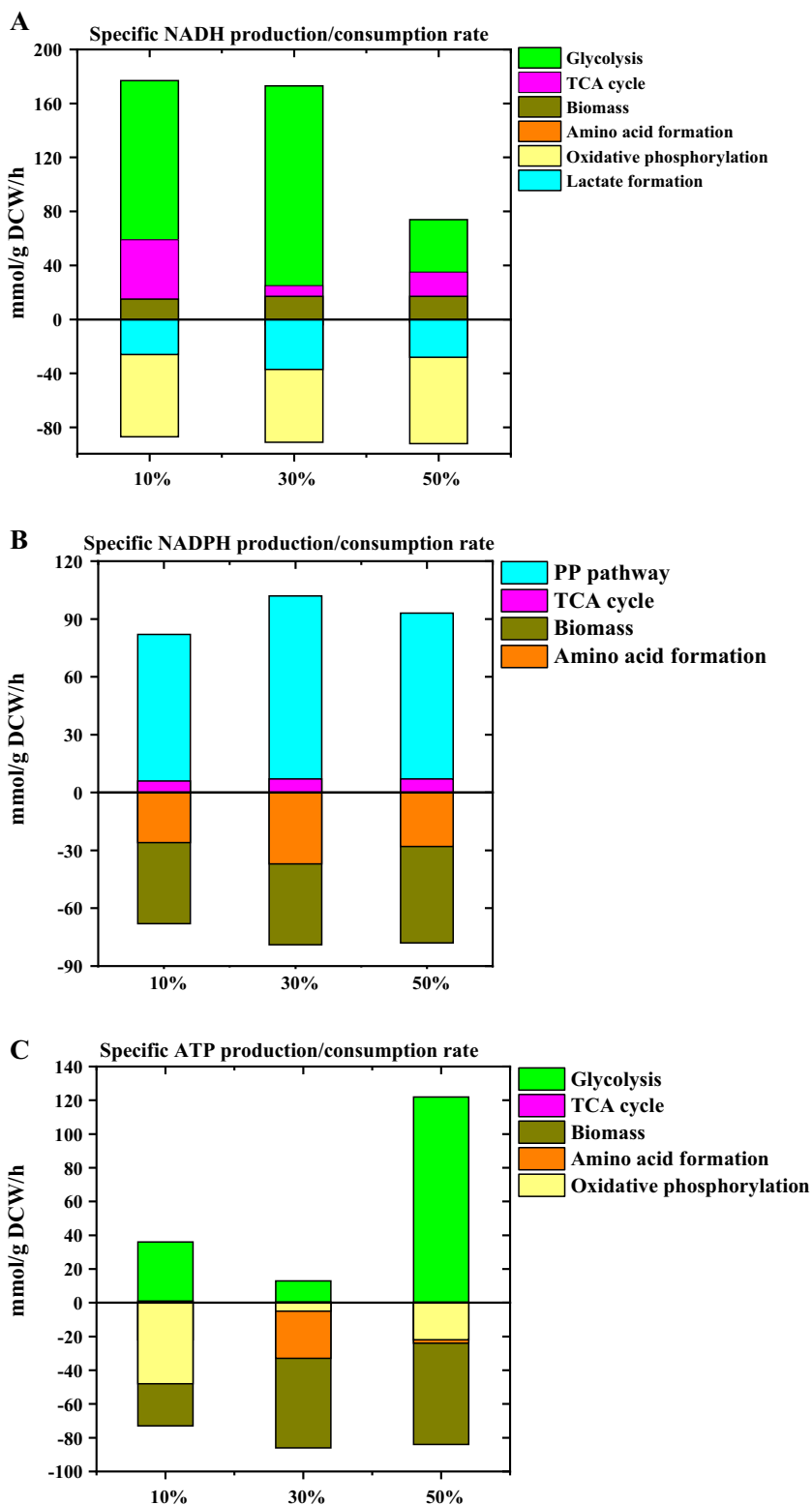
ATP by phosphorylation. Through the glycolysis pathway, a large amount of pyruvate was produced and then lactic acid would be produced with the consumption of NADH, which was consistent with the result that NADH consumption for lactic acid was 26 mmol/(g cell·h) under the 10% DO level condition, lower than that of 30% and 50% DO level, respectively. It has also been reported that NADH acted as a cofactor for the formation of lactic acid from pyruvate by lactate dehydrogenase, and the lower DO was advantageous to promote the activity of lactate dehydrogenase, thereby accumulating lactic acid [26].

The PP pathway was the main source of NADPH and NADPH was primarily used for the synthesis of amino acids and biomass (Fig. 3b). The results obtained in this study showed that the appropriate increase in DO levels (10–30%) will enhance the amount of NADPH required for biomass synthesis. This was consistent with the results of carbon metabolism that the PP pathway was more active and produced more reducing power NADPH under the 30% DO condition. The regulation of DO level during the *E. coli* W3110BL fermentation process actually influenced the intracellular energy level and then affected the intracellular re-oxidation pathway of NADH/NADPH. The decrease in NADH and the increase in NADPH ultimately resulted in a slightly higher oxidation state in both the cytoplasm and mitochondria of the recombinant *E. coli*. From the increase in L-MET concentration and the change in the levels of by-product lactic acid and oxidative phosphorylation, it can be suspected that the NADPH regeneration system plays the key role in material redistribution, consumption of NADH, and increase of the intracellular level of NADPH, thereby promoting synthesis of L-MET in *E. coli*. In addition, the sulfate assimilation also required NADPH for sulfur reduction and approximately 8.5 mol of NADPH is required for the biosynthesis of 1 mol of L-MET in *E. coli* [15]. Therefore, the synthesis of L-MET is not only limited by NADH, but the deficiency of NADPH also affects the synthesis of L-MET. In the subsequent studies, tuning intracellular ATP and NADPH levels and ratios should be considered to further increase L-MET production.

Conclusions

In this study, the FBA method was used for L-MET fermentative production to comprehend the metabolic mechanism of recombinant *E. coli* W3110BL under different DO conditions. The results revealed the producing L-MET flux was higher at 30% DO level and the carbon fluxes for synthesis of L-MET were mainly obtained from the reaction of PEP to OAA but not from the TCA cycle. Additionally, NADPH plays an important role in the synthesis of amino acids and biomass and pentose phosphate pathway was the main

Fig. 3 The specific NADH (a), NADPH (b), and ATP (c) production/consumption rates under different DO levels at exponential growth. Positive values in the graph indicate generation, negative values indicate consumption. All the flux values are normalized to the specific uptake rate of glycerol of 100 mmol/(g cell-h)



source of NADPH which was found to be affected by DO. PP pathway was more active and produced more reducing power

NADPH under the 30% DO, which indicated that the *E. coli* W3110BL fermentation process was actually regulated by

the intracellular energy levels. This study laid a foundation for the production of L-MET with high yield by the genetically engineered *E. coli* strains.

Acknowledgements This research is supported by the National Natural Science Foundation of China (Nos. 31971342 and 31700095).

Compliance with ethical standards

Conflict of interest The authors declare that they have no conflict of interest.

Ethical statement This article does not contain any studies with human participants or animals by any of the authors.

References

- Bai Y, Zhou PP, Fan P, Zhu YM, Tong Y, Wang HB, Yu LJ (2015) Four-stage dissolved oxygen strategy based on multi-scale analysis for improving spinosad yield by *Saccharopolyspora spinosa* ATCC49460. *Microb Biotechnol* 8:561–568. <https://doi.org/10.1111/1751-7915.12264>
- Bellou S, Makri A, Triantaphyllidou IE, Papanikolaou S, Aggelis G (2014) Morphological and metabolic shifts of *Yarrowia lipolytica* induced by alteration of the dissolved oxygen concentration in the growth environment. *Microbiology* 160:807–817. <https://doi.org/10.1099/mic.0.074302-0>
- Chua PS, Salleh AHM, Mohamad MS, Deris S, Omatu S, Yoshioka M (2015) Identifying a gene knockout strategy using a hybrid of the bat algorithm and flux balance analysis to enhance the production of succinate and lactate in *Escherichia coli*. *Biotechnol Bioprocess E* 20:349–357. <https://doi.org/10.1007/s12257-014-0466-x>
- Dubitzky W, Wolkenhauer O, Cho KH, Yokota H (2013) Flux balance. *Analysis*. <https://doi.org/10.1007/978-1-4419-9863-7>
- Garcia A, Ferrer P, Albiol J, Castillo T, Segura D, Pena C (2018) Metabolic flux analysis and the NAD(P)H/NAD(P)(+) ratios in chemostat cultures of *Azotobacter vinelandii*. *Microb Cell Fact* 17:10. <https://doi.org/10.1186/s12934-018-0860-8>
- Georgi T, Rittmann D, Wendisch VF (2005) Lysine and glutamate production by *Corynebacterium glutamicum* on glucose, fructose and sucrose: roles of malic enzyme and fructose-1,6-bisphosphatase. *Metab Eng* 7:291–301. <https://doi.org/10.1016/j.ymben.2005.05.001>
- He L, Xiao Y, Gebreselassie N, Zhang F, Antoniewicz MR, Tang YJ, Peng L (2014) Central metabolic responses to the overproduction of fatty acids in *Escherichia coli* based on ¹³C-metabolic flux analysis. *Biotechnol Bioeng* 111:575–585. <https://doi.org/10.1002/bit.25124>
- Hendry JI, Prasanna CB, Joshi A, Dasgupta S, Wangikar PP (2016) Metabolic model of *Synechococcus* sp. PCC 7002: prediction of flux distribution and network modification for enhanced biofuel production. *Bioresour Technol* 213:190–197. <https://doi.org/10.1016/j.biortech.2016.02.128>
- Hua Q, Yang C, Baba T, Mori H, Shimizu K (2003) Responses of the central metabolism in *Escherichia coli* to phosphoglucose isomerase and glucose-6-phosphate dehydrogenase knockouts. *J Bacteriol* 185:7053–7067. <https://doi.org/10.1128/jb.185.24.7053-7067.2003>
- Huang JF, Liu ZQ, Jin LQ, Tang XL, Shen ZY, Yin HH, Zheng YG (2017) Metabolic engineering of *Escherichia coli* for microbial production of L-methionine. *Biotechnol Bioeng* 114:843–851. <https://doi.org/10.1002/bit.26198>
- Huang JF, Shen ZY, Mao QL, Zhang XM, Zhang B, Wu JS, Liu ZQ, Zheng YG (2018) Systematic analysis of bottlenecks in a multibranch and multilevel regulated pathway: the molecular fundamentals of L-methionine biosynthesis in *Escherichia coli*. *ACS Synth Biol* 7:2577–2589. <https://doi.org/10.1021/acssynbio.8b00249>
- Huang JF, Zhang B, Shen ZY, Liu ZQ, Zheng YG (2018) Metabolic engineering of *E. coli* for the production of O-succinyl-L-homoserine with high yield. *Biotechnol* 8:310. <https://doi.org/10.1007/s13205-018-1332-x>
- Kaushal M, Chary KVN, Ahlawat S, Palabhanvi B, Goswami G, Das D (2018) Understanding regulation in substrate dependent modulation of growth and production of alcohols in *Clostridium sporogenes* NCIM 2918 through metabolic network reconstruction and flux balance analysis. *Bioresour Technol* 249:767–776. <https://doi.org/10.1016/j.biortech.2017.10.080>
- Kim S, Moon DB, Lee CH, Nam SW, Kim P (2009) Comparison of the effects of NADH- and NADPH-perturbation stresses on the growth of *Escherichia coli*. *Curr Microbiol* 58:159–163. <https://doi.org/10.1007/s00284-008-9294-6>
- Kromer JO, Wittmann C, Schroder H, Heinzle E (2006) Metabolic pathway analysis for rational design of L-methionine production by *Escherichia coli* and *Corynebacterium glutamicum*. *Metab Eng* 8:353–369. <https://doi.org/10.1016/j.ymben.2006.02.001>
- Kumar D, Gomes J (2005) Methionine production by fermentation. *Biotechnol Adv* 23:41–61. <https://doi.org/10.1016/j.biotechadv.2004.08.005>
- Li H, Wang BS, Li YR, Zhang L, Ding ZY, Gu ZH, Shi GY (2017) Metabolic engineering of *Escherichia coli* W3110 for the production of L-methionine. *J Ind Microbiol Biotechnol* 44:75–88. <https://doi.org/10.1007/s10295-016-1870-3>
- Lin H, Bennett GN, San KY (2005) Metabolic engineering of aerobic succinate production systems in *Escherichia coli* to improve process productivity and achieve the maximum theoretical succinate yield. *Metab Eng* 7:116–127. <https://doi.org/10.1016/j.ymben.2004.10.003>
- Litsanov B, Brocker M, Bott M (2012) Toward homosuccinate fermentation: metabolic engineering of *Corynebacterium glutamicum* for anaerobic production of succinate from glucose and formate. *Appl Environ Microbiol* 78:3325–3337. <https://doi.org/10.1128/AEM.07790-11>
- Liu ZQ, Dong SC, Yin HH, Xue YP, Tang XL, Zhang XJ, He JY, Zheng YG (2017) Enzymatic synthesis of an ezetimibe intermediate using carbonyl reductase coupled with glucose dehydrogenase in an aqueous-organic solvent system. *Bioresour Technol* 229:26–32. <https://doi.org/10.1016/j.biortech.2016.12.098>
- Liu ZQ, Lu MM, Zhang XH, Cheng F, Xu JM, Xue YP, Jin LQ, Wang YS, Zheng YG (2018) Significant improvement of the nitrilase activity by semi-rational protein engineering and its application in the production of iminodiacetic acid. *Int J Biol Macromol* 116:563–571. <https://doi.org/10.1016/j.ijbio.2018.05.045>
- Liu ZQ, Wu L, Zhang XJ, Xue YP, Zheng YG (2017) Directed evolution of carbonyl reductase from *Rhodospiridium toruloides* and its application in stereoselective synthesis of tert-butyl (3R,5S)-6-chloro-3,5-dihydroxyhexanoate. *J Agril Food Chem* 65:3721–3729. <https://doi.org/10.1021/acs.jafc.7b00866>
- Liu ZQ, Wu L, Zheng L, Wang WZ, Zhang XJ, Jin LQ, Zheng YG (2018) Biosynthesis of tert-butyl (3R,5S)-6-chloro-3,5-dihydroxyhexanoate by carbonyl reductase from *Rhodospiridium toruloides* in mono and biphasic media. *Bioresour Technol* 249:161–167. <https://doi.org/10.1016/j.biortech.2017.09.204>
- Lou F, Li N, Zhao Y, Guo S, Wang Z, Chen T (2016) Effects of overexpression of carboxylation pathway genes and inactivation of

- malic enzymes on malic acid production in *Escherichia coli*. *Chin J Biotechnol* 32:1539–1548. <https://doi.org/10.13345/j.cjb.160101>
25. Manish S, Venkatesh K, Banerjee R (2007) Metabolic flux analysis of biological hydrogen production by *Escherichia coli*. *Int J Hydrogen Energy* 32:3820–3830. <https://doi.org/10.1016/j.ijhydene.2007.03.033>
 26. Matsuoka Y, Kurata H (2017) Modeling and simulation of the redox regulation of the metabolism in *Escherichia coli* at different oxygen concentrations. *Biotechnol Biofuels* 10:183. <https://doi.org/10.1186/s13068-017-0867-0>
 27. Mitsuhashi S (2014) Current topics in the biotechnological production of essential amino acids, functional amino acids, and dipeptides. *Curr Opin Biotechnol* 26:38–44. <https://doi.org/10.1016/j.copbio.2013.08.020>
 28. Mohandas SP, Balan L, Jayanath G, Anoop BS, Philip R, Cubelio SS, Bright Singh IS (2018) Biosynthesis and characterization of polyhydroxyalkanoate from marine *Bacillus cereus* MCCB 281 utilizing glycerol as carbon source. *Int J Biol Macromol* 119:380–392. <https://doi.org/10.1016/j.ijbiomac.2018.07.044>
 29. Muthuraj M, Palabhanvi B, Misra S, Kumar V, Sivalingavasu K, Das D (2013) Flux balance analysis of *Chlorella* sp. FC2 IITG under photoautotrophic and heterotrophic growth conditions. *Photosynth Res* 118:167–179. <https://doi.org/10.1007/s11120-013-9943-x>
 30. Niu K, Zhang X, Tan WS, Zhu ML (2011) Effect of culture conditions on producing and uptake hydrogen flux of biohydrogen fermentation by metabolic flux analysis method. *Bioresour Technol* 102:7294–7300. <https://doi.org/10.1016/j.biortech.2011.05.001>
 31. Park JH, Lee SY (2010) Metabolic pathways and fermentative production of L-aspartate family amino acids. *Biotechnol J* 5:560–577. <https://doi.org/10.1002/biot.201000032>
 32. Shi F, Li K, Huan X, Wang X (2013) Expression of NAD(H) kinase and glucose-6-phosphate dehydrogenase improve NADPH supply and L-isoleucine biosynthesis in *Corynebacterium glutamicum* ssp. *lactofermentum*. *Appl Biochem Biotechnol* 171:504–521. <https://doi.org/10.1007/s12010-013-0389-6>
 33. Sun Y, Guo W, Wang F, Peng F, Yang Y, Dai X, Liu X, Bai Z (2016) Transcriptome and multivariable data analysis of *Corynebacterium glutamicum* under different dissolved oxygen conditions in bioreactors. *PLoS One* 11:e0167156. <https://doi.org/10.1371/journal.pone.0167156>
 34. Usuda Y, Kurahashi O (2005) Effects of deregulation of methionine biosynthesis on methionine excretion in *Escherichia coli*. *Appl Environ Microbiol* 71:3228–3234. <https://doi.org/10.1128/AEM.71.6.3228-3234.2005>
 35. Wang XX, Lin CP, Zhang XJ, Liu ZQ, Zheng YG (2018) Improvement of a newly cloned carbonyl reductase and its application to biosynthesize chiral intermediate of duloxetine. *Process Biochem* 70:124–128. <https://doi.org/10.1016/j.procbio.2018.04.010>
 36. Weiner M, Trondle J, Albermann C, Sprenger GA, Weuster BD (2014) Improvement of constraint-based flux estimation during L-phenylalanine production with *Escherichia coli* using targeted knock-out mutants. *Biotechnol Bioeng* 111:1406–1416. <https://doi.org/10.1002/bit.25195>
 37. Willke T (2014) Methionine production—a critical review. *Appl Microbiol Biotechnol* 98:9893–9914. <https://doi.org/10.1007/s00253-014-6156-y>
 38. Xu JZ, Yang HK, Zhang WG (2018) NADPH metabolism: a survey of its theoretical characteristics and manipulation strategies in amino acid biosynthesis. *Crit Rev Biotechnol* 38:1061–1076. <https://doi.org/10.1080/07388551.2018.1437387>
 39. Xue LL, Chen HH, Jiang JG (2017) Implications of glycerol metabolism for lipid production. *Prog Lipid Res* 68:12–25. <https://doi.org/10.1016/j.plipres.2017.07.002>
 40. Yamamoto S, Sakai M, Inui M, Yukawa H (2011) Diversity of metabolic shift in response to oxygen deprivation in *Corynebacterium glutamicum* and its close relatives. *Appl Microbiol Biotechnol* 90:1051–1061. <https://doi.org/10.1007/s00253-011-3144-3>
 41. Yang JK, Xiong W, Xu L, Li J, Zhao XJ (2015) Constitutive expression of *Campylobacter jejuni* truncated hemoglobin CtrHb improves the growth of *Escherichia coli* cell under aerobic and anaerobic conditions. *Enzyme Microb Technol* 75–76:64–70. <https://doi.org/10.1016/j.enzmictec.2015.04.006>
 42. Yin L, Zhao J, Chen C, Hu X, Wang X (2014) Enhancing the carbon flux and NADPH supply to increase L-isoleucine production in *Corynebacterium glutamicum*. *Biotechnol Bioprocess E* 19:132–142. <https://doi.org/10.1007/s12257-013-0416-z>
 43. Zamboni N, Fendt SM, Ruhl M, Sauer U (2009) ¹³C-based metabolic flux analysis. *Nat Protoc* 4:878–892. <https://doi.org/10.1038/nprot.2009.58>
 44. Zhang X, Shanmugam KT, Ingram LO (2010) Fermentation of glycerol to succinate by metabolically engineered strains of *Escherichia coli*. *Appl Environ Microbiol* 76:2397–2401. <https://doi.org/10.1128/AEM.02902-09>
 45. Zhang X, Zhang D, Zhu J, Liu W, Xu G, Zhang X, Shi J, Xu Z (2019) High-yield production of L-serine from glycerol by engineered *Escherichia coli*. *J Ind Microbiol Biotechnol* 46:221–230. <https://doi.org/10.1007/s10295-018-2113-6>
 46. Zheng YG, Yin HH, Yu DF, Chen X, Tang XL, Zhang XJ, Xue YP, Wang YJ, Liu ZQ (2017) Recent advances in biotechnological applications of alcohol dehydrogenases. *Appl Microbiol Biotechnol* 101:987–1001. <https://doi.org/10.1007/s00253-016-8083-6>
 47. Zheng Y, Chang Y, Zhang R, Song J, Xu Y, Liu J, Wang M (2018) Two-stage oxygen supply strategy based on energy metabolism analysis for improving acetic acid production by *Acetobacter pasteurianus*. *J Ind Microbiol Biotechnol*. <https://doi.org/10.1007/s10295-018-2060-2>
 48. Zhou HY, Wu WJ, Niu K, Xu YY, Liu ZQ, Zheng YG (2019) Enhanced L-methionine production by genetically engineered *Escherichia coli* through fermentation optimization. *3 Biotech*. <https://doi.org/10.1007/s13205-019-1609-8>

Publisher's Note Springer Nature remains neutral with regard to jurisdictional claims in published maps and institutional affiliations.